

# Effect of Niobium on Microstructure and Mechanical Properties of a Hypereutectoid Steel

Ricardo Amorim Pessoa<sup>a</sup>, Rodrigo Rangel Porcaro<sup>a\*</sup> , Luiz Claudio Cândido<sup>a</sup>,

Beatriz Pereda<sup>b</sup>, Beatriz Lopez<sup>b</sup>

<sup>a</sup>Universidade Federal de Ouro Preto, Rede Temática em Engenharia de Materiais, Campus Universitário do Morro do Cruzeiro, 35400-000, Ouro Preto, MG, Brasil.

<sup>b</sup>Ceit-BRTA, Manuel Lardizabal 15, 20018, Donostia/San Sebastián, Spain.

Received: March 17, 2022; Revised: August 05, 2022; Accepted: September 11, 2022

High-carbon steels have been used to high-strength steel wire and strands for prestressing concrete. The necessity of high-strength levels at increasingly larger diameters of wire rods is a technological challenge. Two steels with and without Nb were obtained in a steel mill, submitted to detailed microstructural (previous austenitic grain size, pearlite interlamellar spacing and colony size) and mechanical characterization through tensile tests and hardness. Hot torsion and dilatometry tests were performed to simulate steels processing and to verify the influence of Nb on phase transformation. Adding Nb to steel resulted in a refinement in austenitic grain size and pearlite colonies but had no effect on pearlitic interlamellar spacing. There was a decrease at the start transformation temperature austenite/pearlite and therefore an increase in the hardenability of the Nb-added steel. Finally, Nb addition proved to be a technical and economical way to increase tensile strength and to reduce the variability of the mechanical properties.

**Keywords:** *High-carbon steel, Niobium, Microstructure, Mechanical properties, Wire rod.*

## 1. Introduction

Steel wires and strands for prestressed concrete are manufactured with high-strength, high-carbon steel wire rods, with addition of some alloying elements such as Mn, Cr, Si, to increase the material strength. The increasingly tensile strength requirements at increasingly larger diameters of wire rods is a great challenge, since the simple increase in the amount of carbon above the eutectoid can result in proeutectoid cementite and/or martensite, which could result in failures during cold-drawing or in the final application. The use of Nb in low carbon steels and its effects on microstructure and mechanical properties are well known. However, the use of Nb in hypereutectoid steels and its effects still raises many doubts, including the supposed low solubility of niobium in these steels.

Some works have shown an increase in tensile strength and hardness as a result of Nb addition in hypereutectoid steels<sup>1-3</sup>, and, furthermore, improved ductility of the wire rod during deformation in cold drawing passes have been reported, a result mainly attributed to the reduction of pearlite interlamellar spacing<sup>1,2</sup>. Due to these results, it has been discussed that the solubility of Nb in austenite in high-carbon steel may actually be higher than has been previously reported by some authors<sup>1,2,4</sup>, i.e., as the carbon content increases and other alloying elements such as Mn and Cr are added, there may be a higher amount of Nb in solid solution, which could be attributed to strong interactions between solutes in austenite and non-stoichiometric carbides<sup>2,4</sup>.

A decrease in austenitic grain size has been widely reported by several works due to the Nb adding in high-carbon steels, a result attributed to the solute drag effect and precipitation of Nb(C,N)<sup>2-8</sup>. However, the consequences of the decrease in austenite grain size still presents different conclusions regarding pearlite interlamellar spacing, pearlite colony size and austenite-pearlite start transformation temperature<sup>1-10</sup>. In fact, it depends on the heat treatment (or thermomechanical processing) to which the steel has been subjected. Niobium is a ferrite stabilizer and, in solid solution, reduces the austenitic field, raising the eutectoid temperature, what could reduce the interlamellar spacing<sup>11</sup>. On the other hand, niobium in solid solution is partitioned between austenite and pearlite, slowing the kinetics of pearlite formation, favors the formation of pearlite with greater interlamellar spacing during isothermal heat treatments. Thus, in isothermally transformed steels, niobium can increase the interlamellar spacing in relation to the same steel without niobium<sup>11,12</sup>.

In this context, the effects of Nb in a hypereutectoid steel were evaluated and correlated with microstructural characteristics and mechanical properties. Two materials were manufactured in a steel mill with controlled processing parameters. The results, which includes phase transformation evaluation by dilatometry and hot torsion, allow understanding how the Nb affects the austenitic grain size, pearlite colony size, pearlite interlamellar spacing and austenite/pearlite transformation temperature, as well as the influence on tensile strength and hardness increase of the studied steels.

\*e-mail: [rodrigo.porcaro@ufop.edu.br](mailto:rodrigo.porcaro@ufop.edu.br)

## 2. Materials and Methods

### 2.1. Materials

The studied steels are hypereutectoid such as SWRH82B grade in agreement of JIS G 3506<sup>13</sup> standard, with and without Nb. The materials were manufactured in squared billets of 160 mm using continuous casting machine, hot-rolled up to 13 mm-diameter wire rod and cooled by forced air. The chemical analysis was obtained by optical emission spectrometry and is presented in Table 1, for both steels (82Cr and 82CrNb). It is noteworthy that the only significant difference between the steels is the Nb content, despite being an industrial experiment. Besides this, all the processing parameters were the same for both steels.

### 2.2. Microstructural characterization

The microstructure was evaluated at ¼ diameter wire rod. The steel samples were prepared according to procedures recommended by the ASTM E3<sup>14</sup> standard, followed by chemical etching with Nital 2% in order to reveal the microstructure and an optical microscope was used.

The austenitic grain size was measured at ¼ diameter from the hot-rolled bars with 93.8% and 98.3% area reduction, after water quenching. The samples were prepared and chemical etched with Bechet and Beaujard<sup>15</sup> in order to reveal the prior-austenite grain boundaries. The measurement was performed by average equivalent diameter in agreement of ASTM E112<sup>16</sup> Standard with at least twenty images. An optical microscope was used on CEIT (Spain) facilities.

To allow the measurement of pearlite colony size, a thermal etching by oxidation at 690 °C in a controlled atmosphere furnace (low oxygen partial pressure controlled with continuous argon flux) was performed for 12 min<sup>17</sup>. The samples were analyzed at ¼ diameter wire rod. The measurement was performed by average equivalent diameter in agreement of ASTM E112<sup>16</sup> and ASTM E1382<sup>18</sup> Standards, with at least ten images and the ImageJ software was used.

Wire rod samples at ¼ diameter were chemical etched by Nital 2% and were analyzed by a scanning electron microscope (SEM) with 15,000 x magnification to allow the measurement of pearlite interlamellar spacing. To perform the measurements, those colonies with smaller interlamellar spacing were looked over the micrographs, which are the ones with lamellae perpendicular to the polishing cut<sup>11,19</sup>. Ten different images were used from each steel to measure the pearlite interlamellar spacing. The ImageJ software was used to drawn perpendicular lines to the pearlite lamellae and the number of intercepted cementite lamellae per unit length was determined to obtain the average interlamellar spacing.

### 2.3. Dilatometry

The specimens for dilatometry were machined into solid cylinders with 5 mm-diameter and 10 mm-length, longitudinal to the wire rod and the tests were performed on

**Table 1.** Results of chemical analysis of the studied steels (wt. %).

Steel	C	Mn	Si	Cr	Nb
82Cr	0.82	0.72	0.19	0.22	0.000
82CrNb	0.82	0.74	0.18	0.22	0.023

CEIT facilities. The solubilization temperature was obtained by Thermocalc® and the thermal cycles used to obtain the continuous cooling transformation (CCT) diagrams are presented in Figure 1. The thermal cycles and deformation applied to both materials aimed the austenite conditioning in order to obtain equivalent previous austenitic grain sizes (after some exploratory trials).

The quenched specimens from dilatometry (100 °C/s) were used to obtain the previous austenite grain size with chemical etching Bechet and Beaujard<sup>15</sup>. The other specimens were etched with Nital 2% and an optical microscope was used to obtain the microstructure after dilatometry tests. From the data obtained by dilatometry and confirmed by microstructural analysis, the CCT diagram was drawn for both steels.

### 2.4. Hot torsion test

The specimens were machined into solid cylinders with 7.5 mm diameter and 16.5 mm length, longitudinal to the wire rod and the tests were performed on CEIT facilities. To simulate the hot rolling process, the specimens were austenitized to 1,150 °C, twenty-two torsion passes with deformation of 0.4 ( $\epsilon$ ) were performed, strain rate and interpass time were the same for both steels. Two cycles with different temperatures were utilized: low temperature cycle (LT) with the last pass equal to 980 °C and high temperature cycle (HT) with the last pass equal to 1,030 °C (based on bar hot-rolling schedules (LT) and a variation). Then, two samples were cooled to 910 °C at 10 °C/s, following water quenching to measure the austenitic grain size. The remaining samples were natural air cooled from 910 °C to room temperature in order to observe the recalescence during phase transformation, allowing to recognize the onset of pearlitic transformation. Then, the pearlite interlamellar spacing was measured at least twenty images on CEIT facilities (using SEM and the same procedures applied to the hot-rolled wire rods).

### 2.5. Mechanical tests

For the tensile tests, according to the ISO 6892<sup>20</sup> Standard, the specimens came from straightened wire rod with a gage length about 250 mm and 13 mm-diameter. The tests were performed at room temperature, with a constant speed of 5 mm/min. At least twenty tests were performed on each steel (industrial quality control).

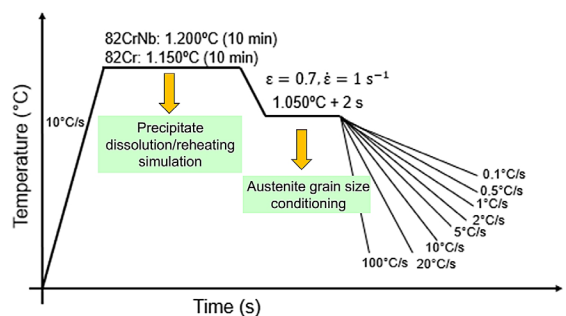


**Figure 1.** Thermal cycles applied to the materials to obtain CCT diagrams with hot deformation and different cooling rates.

The Vickers hardness was measured over the entire diameter (13 mm), equidistant 1 mm from the surface and on two diagonals. The applied load was 1 kgf for 15 s, on CEIT facilities and in agreement of ASTM E92<sup>21</sup> Standard, at least twenty-for points were measured on each steel.

### 3. Results and Discussion

#### 3.1. Microstructural characterization

The typical micrographs of the studied steels are shown in Figure 2, where is possible to observe that, for both materials, the microstructure is fully pearlitic, as expected for this hypereutectoid steel. Martensite and pro-eutectoid cementite were not found during the analysis.

The results of austenitic grain size measurements after 93.8% and 98.3% area reductions for both steels are shown in Figure 3. As can be seen, after the area reduction by hot-rolling, there was a decrease in the average austenitic grain size ( $D_{\gamma}$ ) due to addition of Nb in the steel. This result is in good agreement with several authors, which attributed to the solute drag effect and Nb precipitates might have contributed to restrain the austenitic grain growth in steel<sup>2-8,11,22</sup>.

The pearlite colony size results (wire rod samples) are shown in Table 2 and it is possible to conclude that there was a decrease on the average pearlite colony size when Nb is added to steel, in agreement with previous works<sup>8,10,23</sup>. That is, in general, considering all samples and measurements, the addition of Nb resulted in a decrease of the equivalent circular diameter of around 28%. Analysis of the variance of the data obtained indicated different average values for the two steels. Student's t-tests performed on the paired

data also indicated, with 95% confidence, that there were different means, with  $p < 0.05$ . It is known that the austenite boundaries are preferential sites for pearlite nucleation, thus during austenite continuous cooling, the smaller the prior austenite grains the higher the total grain boundary surface and the higher the preferential sites for pearlite nucleation<sup>7</sup>.

The pearlite interlamellar spacing was not significantly modified by Nb addition as shown in Table 2. These results are in disagreement with previous authors, who showed a decrease in pearlite interlamellar spacing with Nb addition<sup>1,2</sup>. However, other works showed similar results to those obtained here, in which the addition of Nb to a high-carbon steel did not change the pearlitic interlamellar spacing<sup>7</sup>. The cooling rate, consequently the under-cooling, seems to have greater influence on pearlite interlamellar spacing<sup>19,24</sup> than the Nb addition in high-carbon steel, as related by Silva<sup>9</sup>, the increase of the cooling rate resulted in a decrease on pearlite interlamellar spacing. This could be the reason why there is no significant difference in the pearlite interlamellar spacing between the two studied steels, since the cooling rate used after the hot-rolling of the wire rod was the higher possible, probably resulted in maximum refinement of the interlamellar spacing for both steels.

On continuous cooling, the finely precipitated niobium carbide restricts the growth of the austenitic grain, favoring pearlite nucleation and increasing interlamellar spacing. On the other hand, niobium in solid solution reduces the temperature of pearlite formation, by partitioning between austenite and pearlite, reducing the interlamellar spacing. Thus, the balance between the effects of niobium in solid solution (elevation of eutectoid temperature and partitioning) and that of niobium precipitation (refining of the austenitic grain) is what determines the final microstructural characteristics<sup>11,22</sup>. Besides that, as discussed by Mei<sup>11</sup>, considering the Zener<sup>24</sup> model, the effect of niobium in the interlamellar pearlite spacing results of a balance between the changes in the eutectoid temperature and the increase in ferrite-cementite interfacial energy. The balance of these factors depends on the amount of Nb in solid solution, the previous austenitic grain size and the austenite decomposition temperature<sup>11</sup>.

**Table 2.** Average pearlite colony size and pearlite interlamellar spacing for steels 82CrNb and 82Cr. Wire rod samples measured at  $\frac{1}{4}$  diameter.

Steel	Pearlite interlamellar spacing ( $\mu\text{m}$ )	Pearlite colony size ( $\mu\text{m}$ )
82CrNb	$0.12 \pm 0.02$	$9 \pm 6$
82Cr	$0.11 \pm 0.02$	$13 \pm 8$

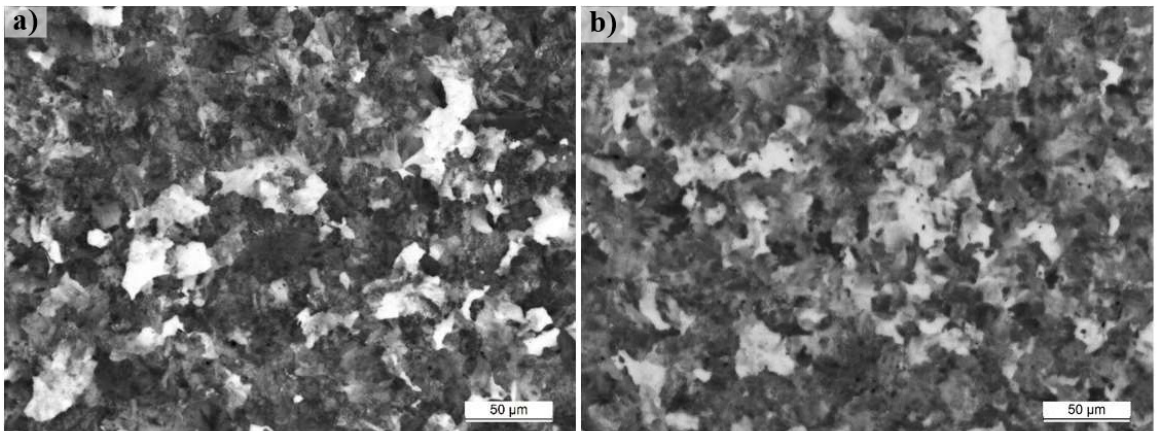


**Figure 2.** Micrographs of wire rod at  $\frac{1}{4}$  diameter etched with Nital 2% and original magnification of 500 x, steels: (a) 82Cr and (b) 82CrNb.

### 3.2. Dilatometry

According to the thermal cycles shown above (Figure 1), using different austenitizing temperatures and performing deformation, it was possible to reach very close previous austenitic grain sizes for both steels as presented in Figure 4. This is a very important result, because the austenite grain size directly influences the start and final phase transformation

temperatures. Therefore, the obtained results at the dilatometer highlights the effects of Nb addition in the phase transformation of high-carbon steels.

The micrographs obtained from the dilatometry samples were very similar for both steel at the same cooling rate (Figure 5). At cooling rates below 5° C/s the microstructure is mainly pearlitic, with little amount of free cementite; above 10 °C/s bainite and martensite formation begins, the

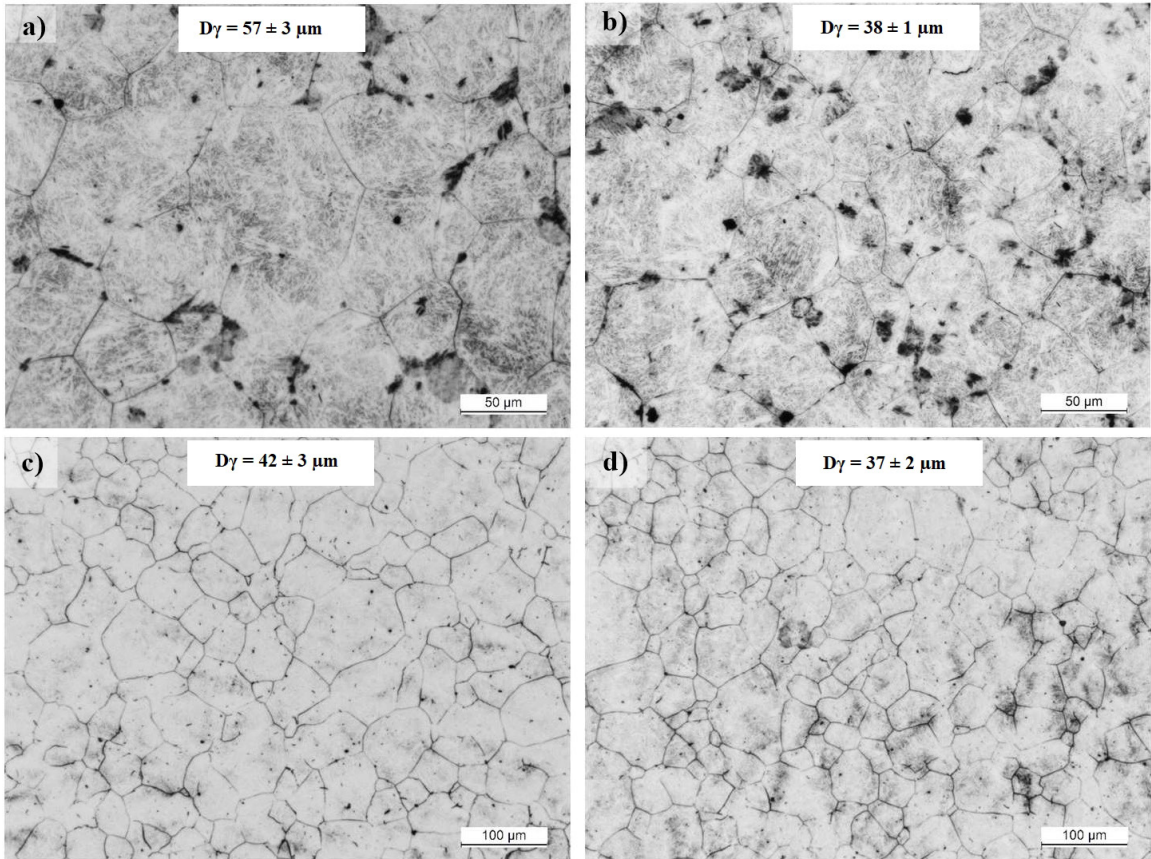


**Figure 3.** Average austenitic grain size of steels: (a) 82Cr and (b) 82CrNb with 93,8% area reduction by hot-rolling; (c) 82Cr and (d) 82CrNb with 98,3% area reduction by hot-rolling – Etched with Bechet-Beaujard.

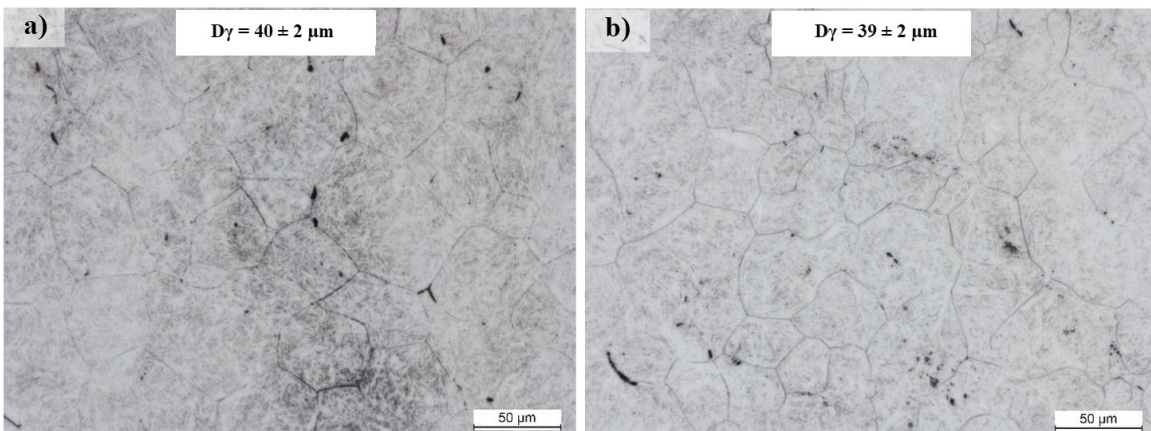


**Figure 4.** Previous austenitic grain size obtained after austenitization in dilatometry, steels: (a) 82Cr at 1,200 °C and (b) 82CrNb at 1,150 °C –  $\varepsilon = 0.7$ . Cooled at 100 °C/s (quenching) and etched with Bechet-Beaujard.

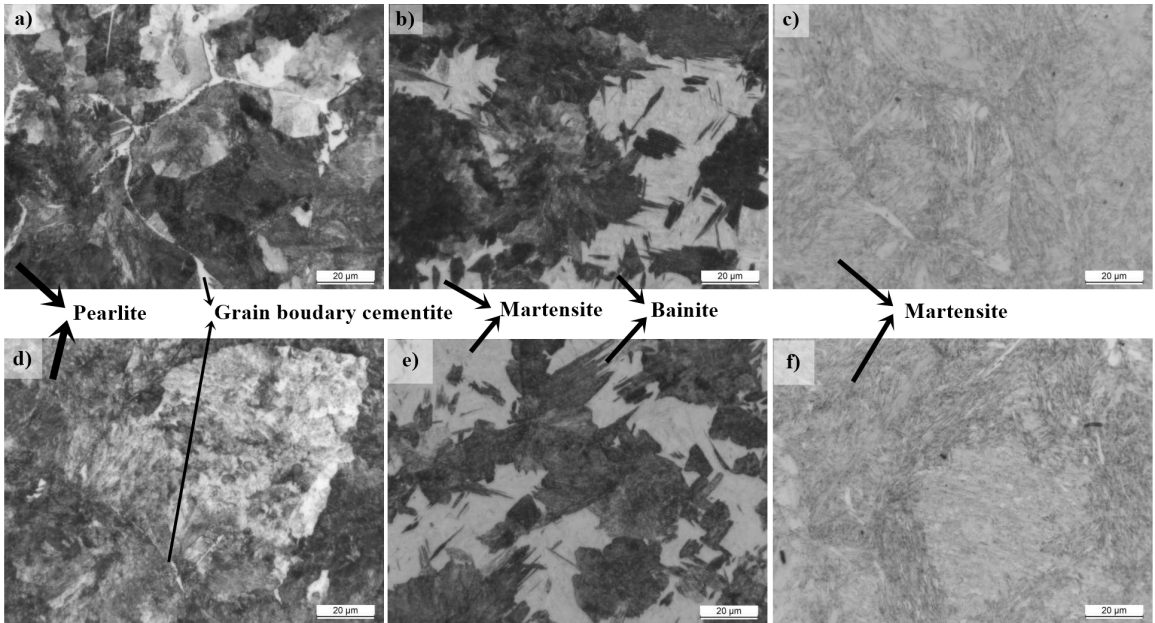


**Figure 5.** Micrographs obtained from dilatometry samples: steel 82Cr (a) 5° C/s, (b) 10 °C/s and (c) 100 °C/s; steel 82CrNb (d) 5° C/s, (e) 10° C/s and (f) 100 °C/s. Etched with Nital 2%.

proportion of martensite increases with the cooling rate until the microstructure is fully martensitic at 100 °C/s.

With the dilatometry data and microstructural analysis, the CCT diagrams were drawn for both studied steels and is in agreement with the microstructural characterization showed before, as shown in Figure 6. It is observed that there is a small decrease at the start and final transformation temperature due to Nb addition in the steel, shifting the CCT diagram to right and down, that results in a small increase in the steel hardenability. However, the hardness values from both steels are similar, with differences within measurement error in most cases.

Fonseca et al.<sup>22</sup> using continuous cooling and a high-carbon steel, reported a delaying at the start and final transformation temperature due to Nb addition in the steel, in agreement with the present work. Rodrigues and Faria<sup>7</sup> studied high-carbon steels and showed that a steel with higher Mn, Si and Nb contents had a smaller previous austenitic grain size and a higher austenite/pearlite start transformation temperature. The authors stated that smaller previous austenitic grain, higher is the total surface area and thus the higher the preferential sites (grain boundary) for pearlite nucleation. Therefore, they concluded that: the smaller the previous austenitic grain size is, the higher is the start transformation temperature austenite/pearlite.

### 3.3. Hot torsion test

The results of austenitic grain size after hot torsion are in agreement of that obtained during hot-rolling as shown above, that is, for the two cycles, LT and HT, when adding Nb to the steel, there was a significant decrease in austenitic grain size, as shown in Figure 7. It is worth noting that when decreasing the deformation temperature, the austenitic grain size was reduced for both steels.

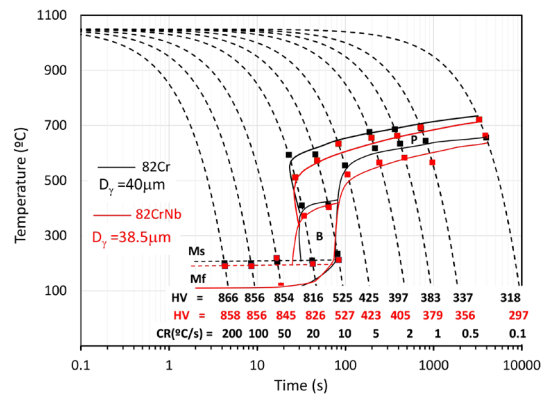


**Figure 6.** CCT diagrams of the 82Cr and 82CrNb steels obtained from similar previous austenitic grain size. Vickers microhardness for each cooling rate are also shown.

Another important result about adding Nb to the high-carbon steel was the higher microstructural homogeneity (austenitic grain size) on both cycles after hot torsion tests (LT and HT). The previous austenitic grain size histograms from samples subjected to the LT cycles are shown in Figure 8, as an example. One can see, in Figure 8b, a narrower range of austenitic grain size of the 82CrNb steel compared to 82Cr steel. The variability reduction due to the Nb addition to the steel was also observed for pearlite colony size and tensile strength results, this will be shown in a later section.

The samples from hot torsion tests cooled at natural air were used to draw the cooling curves as shown in Figure 9, where is observed the recalescence due to pearlitic transformation. As shown before in CCT diagrams, there was a slightly decrease in the pearlitic start transformation temperature when

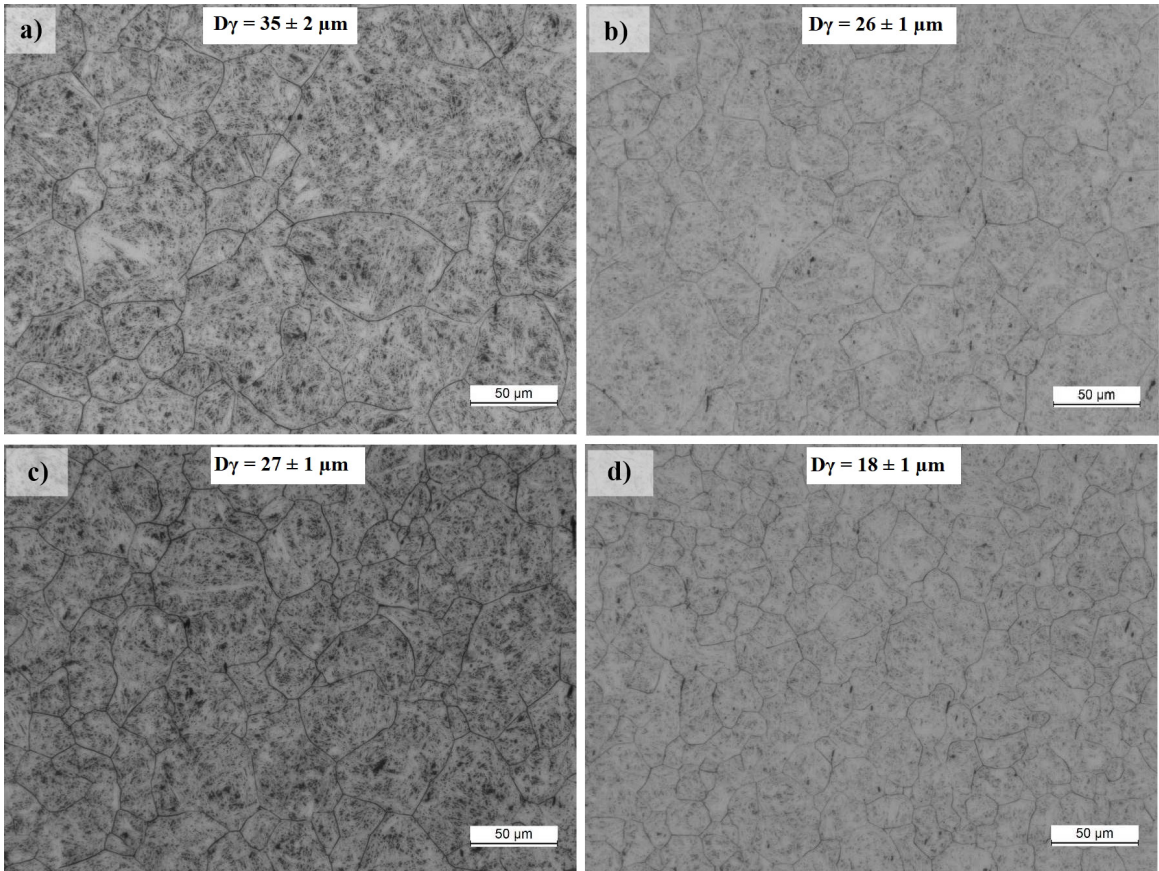


**Figure 7.** Austenitic grain size after hot torsion test: (a) 82Cr and (b) 82CrNb for the HT cycle; (c) 82Cr and (d) 82CrNb for the LT cycle. Quenched samples etched with Bechet-Beaujard.

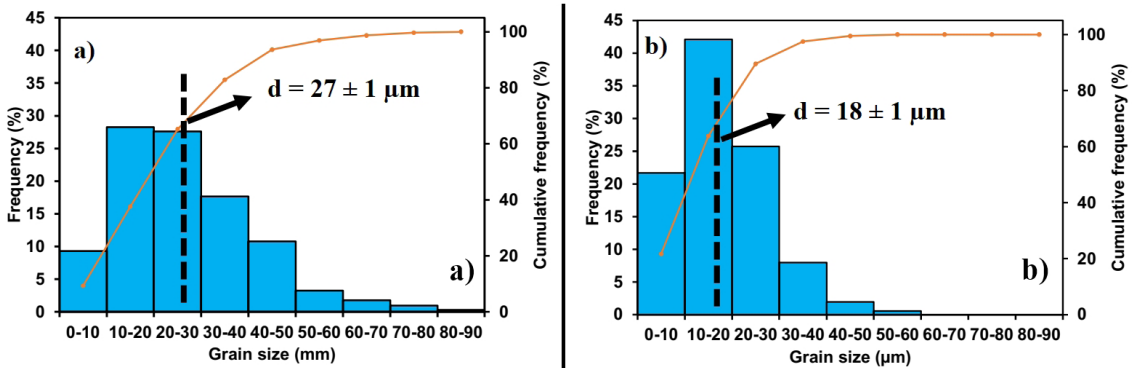


**Figure 8.** Histograms examples of austenitic grain size for the LT cycle during hot torsion test, steels: (a) 82Cr and (b) 82CrNb.

niobium was added to the steel. When observing the HT and LT cycles, no significant difference was noticed. Different from the result reported by Rodrigues and Faria<sup>7</sup>, despite the Nb-added steel having the smaller austenitic grain size, the start transformation temperature was slightly lower than those observed for steel without microalloying. As previously discussed, this could be attributed to partitioning of Nb during the continuous cooling<sup>11</sup>, resulting in a reduction of pearlite formation temperature.

Tian et al.<sup>25</sup>, studying high-carbon steel after deformation obtained different results from those shown here, the authors reported an increase in the pearlitic start temperature transformation with Nb and V addition to the steel. On the other hand, Yong et al.<sup>26</sup> shown similar results to those found here, in which the Nb addition to a high-carbon steel delayed the pearlitic start transformation temperature resulting in a significantly increased hardenability of the material.

The highest pearlite interlamellar spacing ( $S$ ) was observed from the HT cycle in the steel without Nb (Figure 10). That is, for a steel without Nb addition, a higher hot deformation temperature resulted in an increase in austenitic grain, pearlite colonies and pearlite interlamellar spacing. Another highlight is that the steel with Nb addition did not show any influence of the deformation temperature

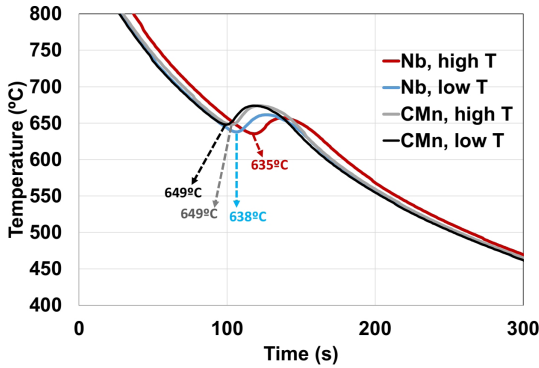


**Figure 9.** Cooling curves with recalescence due to phase transformation, natural air cooled samples after hot torsion tests. Steels 82Cr and 82CrNb.

on the pearlite interlamellar spacing, after the hot torsion tests. Dey et al.<sup>8</sup> found different results, with a high-carbon steel after hot deformation, they reported that an increase in the austenitization temperature resulted in a decrease in pearlite interlamellar spacing. Another work<sup>27</sup> found that, for eutectoid steels, with the same previous austenitic grain size, subjected to continuous cooling, interlamellar spacing was smaller with the Nb-addition.

### 3.4. Mechanical tests

The results of tensile strength, percent reduction of area and Vickers hardness from the wire rod samples are shown in Table 3. There was a consistent increase in the tensile strength when Nb was added to the steel. These results are attributed to the effects of Nb in decreasing the average austenitic grain size, decrease in the pearlite colonies size and increase in

**Table 3.** Tensile strength, area reduction and Vickers hardness of both studied steels (wire rod samples).

Steel	Tensile strength (MPa)	Area reduction (%)	Hardness (HV)
82CrNb	$1,171 \pm 7$	$50 \pm 2$	$345 \pm 4$
82Cr	$1,142 \pm 9$	$48 \pm 2$	$337 \pm 5$

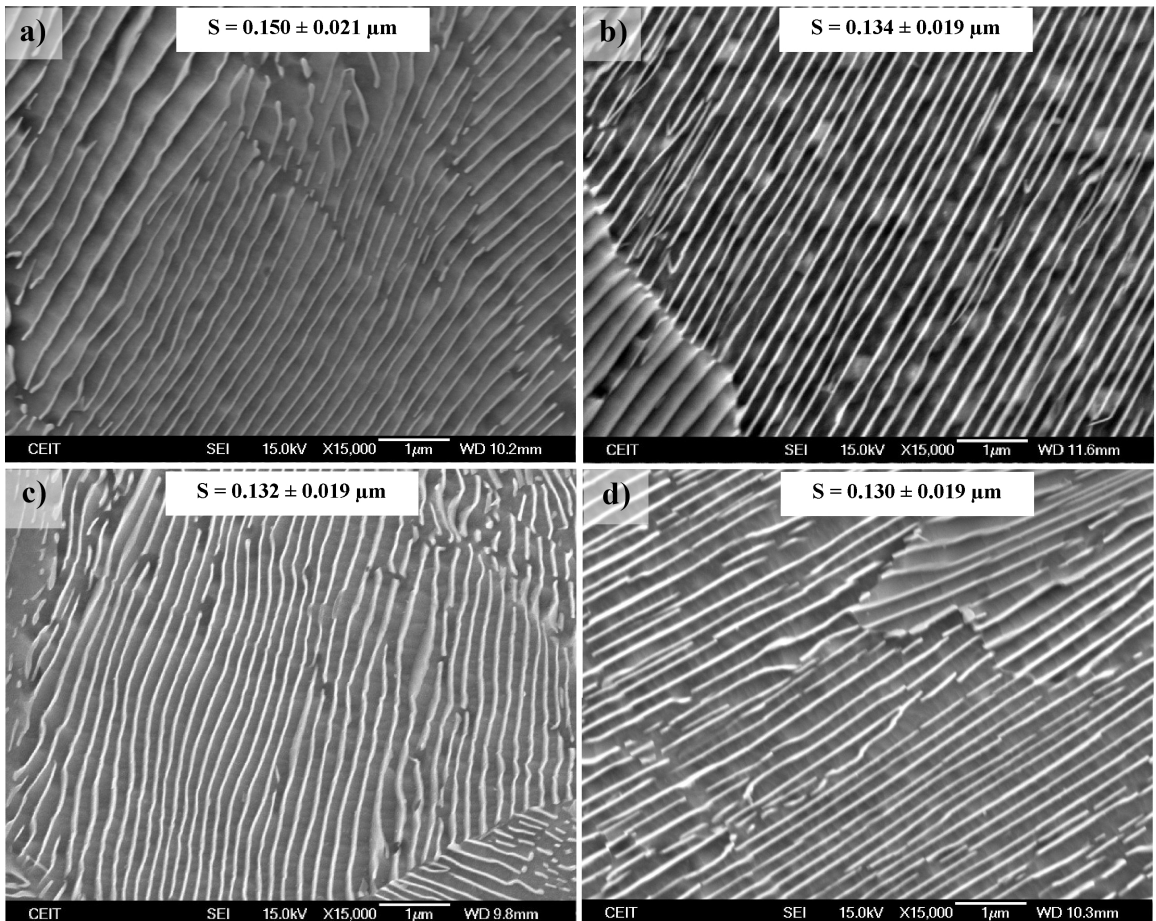


**Figure 10.** Pearlite interlamellar spacing from natural air cooled samples after hot torsion test: cycle HT (a)82Cr and (b)82CrNb; cycle LT (c)82Cr and (d)82CrNb.

hardenability, however it is likely that some contribution from precipitation of Nb(C,N) has occurred<sup>2-8,10,23</sup>. Although the difference about 30 MPa in tensile strength between the two steels is apparently low, analysis of the variance of the data obtained indicated different average values for the two steels. Student's t-tests performed on the paired data also indicated, with 95% confidence, that there were different means, with  $p < 0.05$ . The increase in the steel hardness of 8 HV is in agreement with the increase in tensile strength. On the other hand, despite having shown an increase in the area reduction, for Nb-added steel, the difference was low and statistically not significant.

The increase on the tensile strength and the lower variability resulting from Nb addition to the steel significantly reduces the possibility of obtaining results below the minimum required by customers, which could result in wire rod loss due to scrap. During steel mill production, the Nb addition increased the steel cost by 1.81%, however there was a significant increase in the metallic yield. In general, there was a reduction in the cost of the final product (wire rod) by approximately 9%, which makes the addition of Nb to this steel a viable solution from a technical and economic point of view.

#### 4. Conclusions

Two hypereutectoid steels were manufactured in a steel mill plant, with and without Nb addition, and with controlled process parameters. The microstructure and mechanical properties characterization was performed and the hot-rolling was simulated by hot torsion test, including dilatometry tests to investigate the effects of Nb addition on phase transformation. The following conclusions can be drawn:

- The Nb addition to high-carbon steel resulted in a decrease in the austenitic grain size, with or without hot deformation. A higher microstructural homogeneity was also obtained in the Nb-added steel.
- The smaller austenitic grain size resulted in an average decrease of 28% in pearlite colony size as a result of Nb addition to the steel.
- There was no significant difference in pearlite interlamellar spacing with the Nb addition in the material manufactured in a steel mill plant. The hot torsion tests results indicated that the final hot-rolling temperature has greater effect than the Nb content on the interlamellar spacing.
- The dilatometry and hot torsion test results showed that Nb addition slightly increased the steel hardenability, decreasing the pearlite start transformation temperature.
- The Nb addition to the steel resulted in an increase of the tensile strength and hardness, besides a reduction in variability of these mechanical properties. The increase in steel mechanical strength was attributed to a smaller average pearlite colony size, an increase of the hardenability and a probable precipitation of Nb carbides/nitrides.
- The technical and economic analysis in a steel mill showed that Nb-added high-carbon steel is a viable solution to the production of hot-rolled wire rod. The increase in alloy costs was 1.81%, followed by

an increase in the metallic yield which represented a reduction in the average costs of the wire rod in approximately 9%.

#### 5. Acknowledgments

The authors thank Gerdau and CBMM for their financial support, as well as CEIT and UFOP for the steel characterization tests and technical support.

#### 6. References

1. Jansto SG. MicroNiobium® steelmaking alloy approach in 1080 wire rod. *Iron Steel Technol.* 2014;82(1):42-6.
2. Jarreta DD. Niobium micro-alloyed high carbon steel wires: innovative solution for bridges and infrastructure. *SEAIISI Quarterly J.* 2017;6(2):29-36.
3. Moreira LP. Influência de tratamentos térmicos na resistência à fadiga e ao desgaste de um aço alto carbono microalloyado ao Nb e V de aplicação ferroviária [dissertation]. Ouro Preto: Rede Temática de Engenharia de Materiais; 2019. [Portuguese]
4. Ray A. Niobium microalloyed rail steels. *Mater Sci Technol.* 2017;33(14):1584-600.
5. Zhang F, Zhao Y, Tan Y, Ji X, Xiang S. Study on the nucleation and growth of pearlite colony and impact toughness of eutectoid steel. *Metals (Basel).* 2019;9(11):1-13.
6. Uranga P, Bastos F, Pereda B, López B, Rodrigues-Ibabe JM, Rebellato M. Revisiting the role of Nb microalloying in medium-high carbon steels. *Mater Sci Technol.* 2018;1148-56.
7. Rodrigues KF, Faria GL. Characterization and prediction of continuous cooling transformations in rail steels. *Mater Res.* 2021;24(5):1-12.
8. Dey I, Chandra S, Saha R, Ghosh SK. Effect of Nb micro-alloying on microstructure and properties of thermomechanically processed high carbon pearlitic steel. *Mater Charact.* 2018;140:45-54.
9. Silva FA. Efeito do resfriamento controlado após laminação a quente nas propriedades mecânicas e na microestrutura de um fio-máquina de aço alto carbono com cromo [dissertation]. Belo Horizonte: Universidade Federal de Minas Gerais; 2007. [Portuguese]
10. Porcaro RR, Faria GL, Godefroid LB, Apolonio GR, Cândido LC, Pinto ES. Microstructure and mechanical properties of a flash butt welded pearlitic rail. *J Mater Process Technol.* 2019;270:20-7.
11. Mei PR. Efeito do Nióbio no espaçamento interlamelar da perlita. In: Congresso Anual da ABM; 1987 Oct; Salvador, BA. Proceedings. São Paulo: ABM; 1987. p. 289-304. [Portuguese]
12. Rezende AB, Fernandes FM, Fonseca ST, Farina PFS, Goldenstein H, Mei PR. Effect of alloy elements in time temperature transformation diagrams of railway wheels. In: Defect and Diffusion Forum. Proceedings. Switzerland: Trans Tech Publications Ltd; 2020. p. 11-20. <http://dx.doi.org/10.4028/www.scientific.net/DDF.400.11>.
13. JIS: Japanese Industrial Standard. JIS G 3506: high carbon steel wire rods. Tokyo: JIS; 2017.
14. ASTM: American Society for Testing and Materials. ASTM E3: standard guide for preparation of metallographic specimens. West Conshohocken: ASTM; 2017.
15. Bechet S, Beaujard L. New reagent for the micrographical demonstration of the austenite grain of hardened or hardened-tempered steels. *Rev Metall.* 1955;830-6.
16. ASTM: American Society for Testing and Materials. ASTM E112: standard test methods for determining average grain size. West Conshohocken: ASTM; 2013.
17. Faria GL, Moreira PS, Porcaro RR, Barboza APM, Silva TCV. Development of an oxidation contrast method for pearlite colony

- revelation in eutectoid steels. *Metallography. Microstructure and Analysis*. 2021;10(5):589-600.
18. ASTM: American Society for Testing and Materials. ASTM E1382: standard test methods for determining average grain size using semiautomatic and automatic image analysis. West Conshohocken: ASTM; 2015.
  19. Krauss G. *Steels: processing, structure and performance*. Materials Park, Ohio: ASM International; 2005.
  20. ISO: International Organization for Standardization. ISO 6892: metallic materials – tensile testing. Switzerland: ISO; 2016.
  21. ASTM: American Society for Testing and Materials. ASTM E92: standard test methods for Vickers hardness and Knoop hardness of metallic materials. West Conshohocken: ASTM; 2017.
  22. Fonseca ST, Rezende AB, Oliveira CR, Minucucci DJ, Mei PR. Physical simulation as a tool to evaluate the complex microstructure of microalloyed railroad wheels. *Journal of Materials, Processing and Design*. 2020;4:20-35.
  23. Aranda MM, Kim B, Rementeria R, Capdevila C, De Andrés CG. Effect of prior austenite grain size on pearlite transformation in a hypoeutectoid Fe-C-Mn steel. *Metall Mater Trans, A Phys Metall Mater Sci*. 2014;45(4):1778-86.
  24. Zener C. *Kinetics of the decomposition of austenite*. New York: American Institute of Mining and Metallurgical Engineers; 1946.
  25. Tian J, Wang H, Zhu M, Zhou M, Zhang Q, Sue X, et al. Improving mechanical properties in high-carbon pearlitic steels by replacing partial V with Nb. *Mater Sci Eng A*. 2022;834:1-12.
  26. Yong QL, Zhang ZY, Sun XJ, Cao JC, Li ZD. Effect of dissolved niobium on eutectoid transformation behavior. *J Iron Steel Res Int*. 2017;24(9):973-8.
  27. Mei PR, Silva ALC. *Aços e ligas especiais*. 4. ed. São Paulo: Blucher; 2021.